Supporting Information for

Evaluating Solvothermal and Mechanochemical Routes towards the Metal-Organic Framework Mg_2(*m*-dobdc)

Elena Y. Chen,[a,†] Ruth M. Mandel,[a,†] Phillip J. Milner[a,*]

[a]Department of Chemistry and Chemical Biology, Cornell University, Ithaca, NY, 14850, United States

*pjm347@cornell.edu

[†]Contributed equally.

Table of Contents:

1. General procedures.

All reagents and materials, including 2,4-dihydroxybenzoic acid (97%, Oakwood Chemical), $KHCO_3$ (99%, Oakwood Chemical), CO_2 (bone dry, Airgas), concentrated HCl (36.5–38.0%, J.T. Baker), deuterated dimethyl sulfoxide (DMSO-d_6, 99%, Cambridge Isotope Laboratories), $Mg(NO_3)_2{\cdot}6H_2O$ (98–102%, Beantown Chemical), $Mg(OAc)_2{\cdot}4H_2O$ (98–102%, Alfa Aesar), MgO (97+%, Oakwood Chemical), *N*,*N*-dimethylformamide (DMF, 99.8%, Fischer Scientific), *N*,*N*-dimethylacetamide (DMA, 99%, Acros Organics), methanol (MeOH, 99.8%, Fischer Scientific), ethanol (EtOH, 95%, Fischer Scientific), NaOH (pellet USP 98%, Oakwood Chemical), acetone (99.5%, Petroleum and Solvents), DCl (35 wt % solution in D_2O, 99 atom % D, Sigma-Aldrich), *N*,*N*-diisopropylethylamine (Hünig's base, 99%, Sigma-Aldrich), triethylamine (Et_3N, 99.5%, Sigma-Aldrich), and 2,6-lutidine (redistilled 99+%, Signa-Aldrich) were purchased from commercial vendors and used without further purification, unless otherwise specified.

Infrared (IR) spectra were collected on a Bruker Tensor II IR spectrometer equipped with a diamond Attenuated Total Reflectance (ATR) attachment. Surface area data were collected on a Micromeritics ASAP 2460 or 2020 gas sorption analyzer using ultrapure N_2 (99.999%) and a liquid N_2 bath. Brunauer-Emmett-Teller (BET) and Langmuir surface areas were determined by linear least squares regression analysis using the linearized forms of the BET and Langmuir equations, respectively. CO_2 adsorption isotherms were collected on a Micromeritics ASAP 2020 gas sorption analyzer. A circulating water bath was used for isotherms carried out at 30 °C, 40 °C, and 50 °C. Prior to gas adsorption measurements, MOFs were activated at 180 °C (ramp rate of 1 °C/min) under high vacuum (<10 μbar) for 24 h on a Micromeritics Smart VacPrep system. We have consistently observed lower surface areas when faster ramp rates are employed to activate Mg_2(*m*-dobdc), likely due to partial pore collapse if it is heated too quickly. Powder X-ray diffraction (PXRD) patterns were collected on a Rigaku Ultima IV diffractometer or a Bruker D8 Advance ECO diffractometer equipped with a Cu Kα source (λ = 1.5406 Å). Experimental PXRD patterns were baseline corrected using OriginPro. ^{1}H and ^{13}C NMR data were collected on a Bruker INOVA 500 or 400 MHz spectrometer and are referenced to residual solvent. Thermogravimetric decomposition profiles were collected on a TA Instruments TGA Q5000 thermogravimetric analyzer (TGA) using a temperature ramp of 3.00 °C/min from 40.00 °C to 600.00 °C under an atmosphere of flowing N_2 (flow rate of 60 mL/min). Scanning electron microscopy (SEM) images were taken at 1.0 kV using a Zeiss Gemini 500 scanning electron microscope. The powder samples were immobilized on carbon tape mounted on an aluminum stub. The samples were blown using compressed air to remove excess material not stuck to the tape and then were coated with a carbon layer.

CO_2 adsorption data were fit using the dual-site Langmuir-Freundlich model (eq. S1), where *Q(P)* is the predicted uptake *Q* at pressure *P* in mmol/g, Q_{sati} is the saturation pressure of binding site *i* in mmol/g, b_i is the Langmuir parameter of site *i*, v_i is the Freundlich parameter of site *i*, $-S_i$ is the entropy of binding site *i* in J/mol•K, R is the ideal gas constant, E_i is the enthalpy of adsorption for binding site *i* in kJ/mol, and *T* is the temperature in K. The isotherms were fit with v_1 and v_2 set as 1 (dual-site Langmuir model). Fits were obtained using Solver in Microsoft Excel.

$$Q(P) = \frac{Q_{sat1}(b_1P)^{v_1}}{1+(b_1P)^{v_1}} + \frac{Q_{sat2}(b_2P)^{v_2}}{1+(b_2P)^{v_2}}; b_i = e^{\left(\frac{-S_i}{R}\right)\left(\frac{1000 \cdot E_i}{RT}\right)}$$ eq. S1

Heats of adsorption were calculated using the Clausius-Clapeyron equation (eq. S2), where P_Q are pressure values corresponding to the same loading Q, ΔH_{ads} is the differential enthalpy of adsorption in kJ/mol, R is the ideal gas constant, T is the temperature in K, and c is a constant. Fits over a range of Q values were obtained using Mathematica.

$$\ln\left(P_Q\right) = \left(\frac{\Delta H_{ads}}{R}\right)\left(\frac{1}{T}\right) + c$$ eq. S2

Non-competitive selectivities (S) were determined using eq. S3, where P_{CO_2} is 150 mbar, P_{N_2} is 750 mbar, Q_{CO_2} is the uptake at 150 mbar of CO_2, and Q_{N_2} is the uptake at 750 mbar of N_2.

$$S = (Q_{CO_2}/Q_{N_2})/(P_{CO_2}/P_{N_2})$$ eq. S3

General procedure for digesting MOFs.

Mg_2(*m*-dobdc) samples were digested by suspending ~5 mg of MOF in DMSO-d_6 (~0.5 mL) in a vial and adding concentrated DCl in D_2O (5 drops). The suspension was sonicated until homogeneous and analyzed by ^{1}H NMR.

2. Synthesis of H$_4$*m*-dobdc.

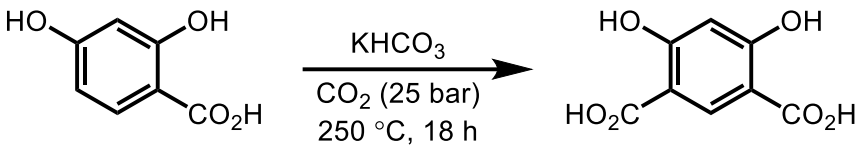

Figure S1. Synthesis of H$_4$*m*-dobdc.

This procedure was adapted from the literature.[1] 2,4-dihydroxybenzoic acid (5.50 g, 35.7 mmol, 1.00 equiv.) and $KHCO_3$ (11.5 g, 115 mmol, 3.22 equiv.) were ground separately using a mortar and pestle and dried in a vacuum oven at 60 °C for 18 h. Once cooled to room temperature, the solids were thoroughly mixed together and sealed in a Parr reactor equipped with a pressure gauge and an internal temperature probe. The Parr reactor was pressurized with CO_2 to 25 bar and subsequently vented to the atmosphere. This process was repeated a total of three times. The Parr reactor was then pressurized a final time with CO_2 to 25 bar, sealed, and heated to 250 °C as measured by the internal temperature probe in a sand bath for 18 h. The final pressure of CO_2 in the Parr reactor reached 40 bar when fully heated. Note: in our hands, inconsistent results were obtained when an external thermometer was employed to monitor the reaction temperature. After 18 h, the Parr reactor was allowed to cool to room temperature and vented. Deionized (DI) water (500 mL) was added to the Parr reactor, and the mixture was sonicated until homogeneous. The solution was then acidified with concentrated HCl until pH < 1, at which time a pale pink solid precipitated from solution. The solid was collected by vacuum filtration, washed with DI water, and dried overnight to yield H$_4$*m*-dobdc as a cream-colored powder (5.69 g, 80% yield). ^{1}H NMR (500 MHz, DMSO-d_6): δ 8.30 (s, 1 H), 6.42 (s, 1 H) ppm (the carboxylic acid and phenol O–H resonances could not be reliably observed). This spectrum is consistent with that reported in the literature.[1] ^{13}C NMR (400 MHz, DMSO-d_6): δ 173.95, 166.58, 135.17, 106.01, 103.26 ppm. ATR IR (powder, cm^{-1}): 3017, 1644, 1596, 1462, 1421, 1327, 1271, 1241, 1157, 1129, 1063, 934, 894, 855, 841, 783, 739, 695, 603, 524.

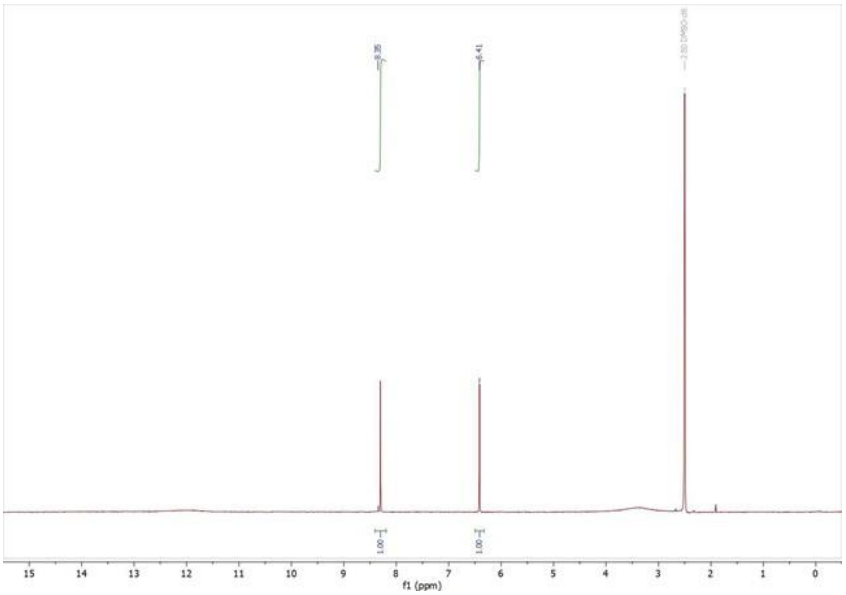

Figure S2. ^{1}H NMR (500 MHz, DMSO-d_6) spectrum of H_4*m*-dobdc used in this work.

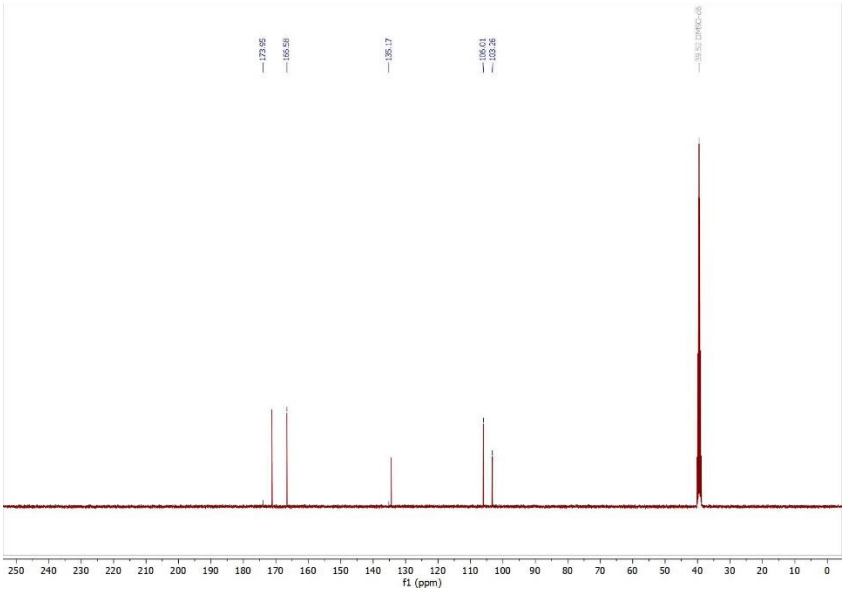

Figure S3. ^{13}C NMR (400 MHz, DMSO-d_6) spectrum of H_4*m*-dobdc used in this work.

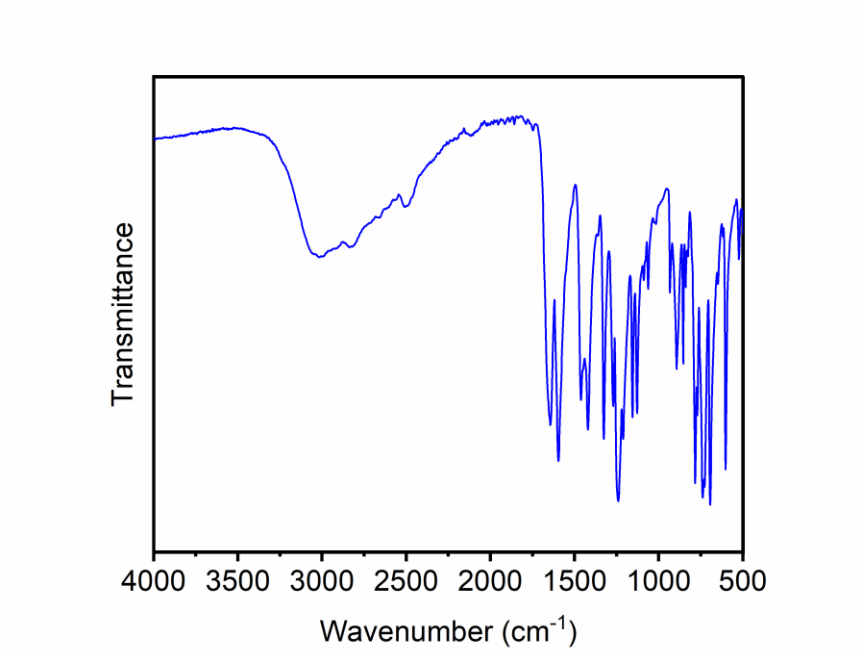

Figure S4. ATR IR spectrum of H_4*m*-dobdc used in this work.

3. Synthesis and characterization of solvothermal (ST) Mg_2(*m*-dobdc)-ST.

a. Optimization of solvothermal Mg_2(*m*-dobdc)-ST synthesis.

Procedure for small-scale solvothermal reactions (Table S1). H_4*m*-dobdc (29.7 mg, 0.150 mmol, 1.00 equiv.) and $Mg(NO_3)_2 \cdot 6H_2O$ (96.2 mg, 0.375 mmol, 2.50 equiv.) or $Mg(OAc)_2 \cdot 4H_2O$ (80.5 mg, 0.375 mmol, 2.50 equiv.) were added to a 15 mL screw-cap reaction tube equipped with a stir bar along with the corresponding solvent mixtures indicated in Table S1 (5 mL). NaOH (1.00–6.00 equiv. relative to H_4*m*-dobdc) was also added as indicated in Table S1. The tube was capped, and the reaction mixture was allowed to stir at 700 rpm at the temperature indicated in Table S1 for 24 h or until solid was observed in the reaction tube. If no solid formed after 72 h, the reaction was stopped. If solid formed, the reaction mixture was allowed to cool to room temperature and filtered, and the resulting solid was thoroughly rinsed with methanol. PXRD patterns were collected on the freshly washed solids. The tested conditions are based on those previously reported for the solvothermal preparations of M_2(dobdc) MOFs.[2–5]

Table S1. Small-scale solvothermal Mg_2(*m*-dobdc)-ST synthesis attempts. rt = room temperature.

Condition	Mg Salt	Solvent	NaOH added	Temperature	Result
1	$Mg(NO_3)_2 \cdot 6H_2O$	1:1 DMF:MeOH	-	120 °C	Pink solid, Mg_2(*m*-dobdc)
2		1:1 DMF:EtOH	-	120 °C	Pink solid, Mg_2(*m*-dobdc)
3		1:1 DMF:H_2O	-	120 °C	No solid
4		1:1 DMA:MeOH	-	120 °C	Pink solid, Mg_2(*m*-dobdc)
5		1:1 DMA:EtOH	-	120 °C	No solid
6		1:1 DMA:H_2O	-	120 °C	No solid
7		2:1 DMF:MeOH	-	120 °C	Brown, amorphous solid
8	$Mg(OAc)_2 \cdot 4H_2O$	H_2O	-	70 °C	No solid
9		1:1 THF:H_2O	-	70 °C	No solid
10		1:1 EtOH:H_2O	-	70 °C	No solid
11		EtOH	-	70 °C	No solid
12		H_2O	1.00 equiv.	rt	No solid
13			2.00 equiv.	rt	No solid
14			3.00 equiv.	rt	Wrong phase
15			4.00 equiv.	rt	Wrong phase
16			5.00 equiv.	rt	No solid
17			6.00 equiv.	rt	No solid

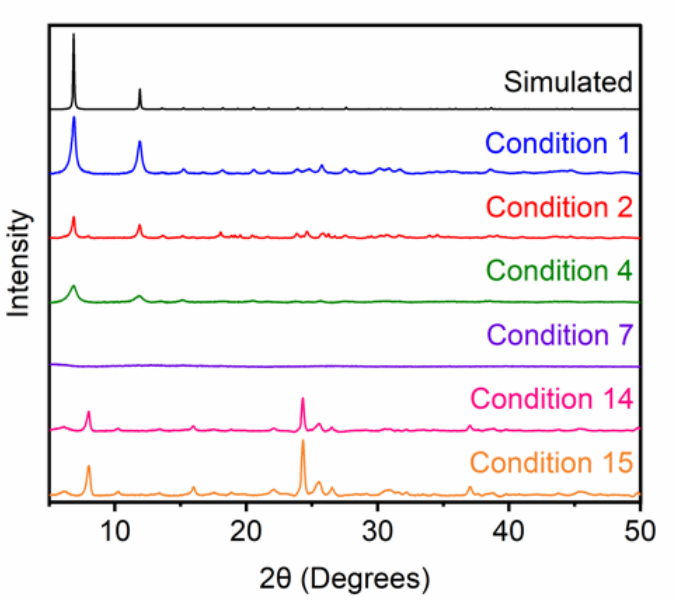

Figure S5. PXRD patterns (λ = 1.5406 Å) of solvothermal Mg_2(*m*-dobdc)-ST synthesis attempts. Condition 1 (Table S1) yielded the highest quality material and thus was employed for the large-scale synthesis of Mg_2(*m*-dobdc)-ST under solvothermal conditions. The simulated pattern based on the previously reported single-crystal X-ray diffraction structure of the isostructural framework Co_2(*m*-dobdc) is included for reference.[6]

b. Synthesis of large-scale solvothermal Mg_2(*m*-dobdc)-ST.

Procedure for large-scale solvothermal synthesis. H_4*m*-dobdc (0.558 g, 2.82 mmol, 1.00 equiv.) and $Mg(NO_3)_2{\cdot}6H_2O$ (1.81 g, 7.05 mmol, 2.50 equiv.) were added to a 1 L screw-cap, high-pressure reaction vessel equipped with a stir bar. DMF (135 mL) and methanol (135 mL) were added, and the reaction vessel was sealed. The flask was placed in a silicone oil bath and heated to 120 °C with stirring at 700 rpm. The reaction mixture was allowed to stir at 120 °C for 48 h. At this time, the reaction mixture was cooled to room temperature and filtered. The resulting solid was rinsed with DMF and transferred to a 1 L Pyrex jar. DMF (500 mL) was added, and the jar was placed in an oven that had been pre-heated to 120 °C. The jar was allowed to stand at 120 °C for 24 h. At this time, the jar was allowed to cool to room temperature, and the DMF was decanted. Fresh DMF (500 mL) was added, and the jar was returned to the oven. This process was repeated for a total of three hot DMF washes. After decanting the third DMF wash, methanol (500 mL) was added to the jar, and the jar was placed in an oven that had been pre-heated to 60 °C. The soaking process outlined above was repeated for a total of three hot MeOH washes. After decanting the third MeOH wash, acetone (500 mL) was added to the jar, and the jar was allowed to stand at room temperature. The soaking process outlined above was repeated for a total of three room temperature acetone washes. After the final acetone wash was decanted, the light-brown solid was transferred to a 10 mL Schlenk flask and activated under high vacuum (<100 mbar) at 180 °C in a sand bath (ramp rate 1 °C/min) for 24 h to yield activated Mg_2(*m*-dobdc)-ST (470 mg, 69% yield)

as a tan-colored solid. Approximately 50 mg of MOF was transferred to a Micromeritics ASAP tube and activated under high vacuum (<10 μbar) at 180 °C for 24 h prior to gas sorption measurements.

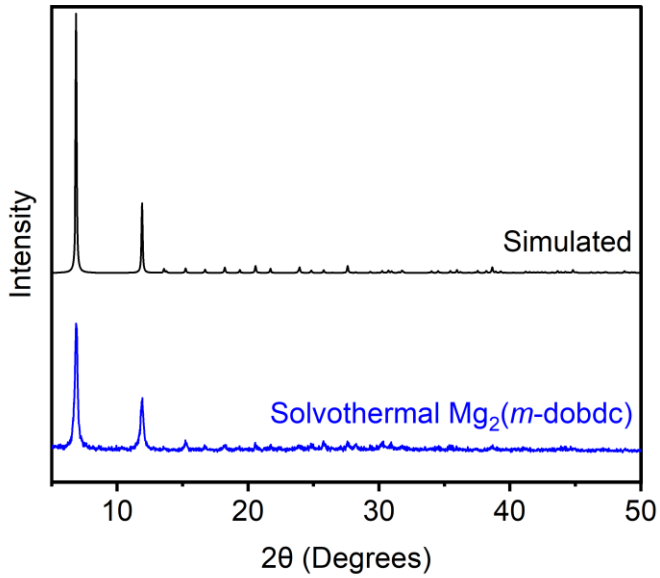

Figure S6. PXRD pattern (λ = 1.5406 Å) of acetone-solvated Mg_2(*m*-dobdc)-ST prepared under solvothermal conditions. The simulated pattern based on the previously reported single-crystal X-ray diffraction structure of the isostructural framework Co_2(*m*-dobdc) is included for reference.[6]

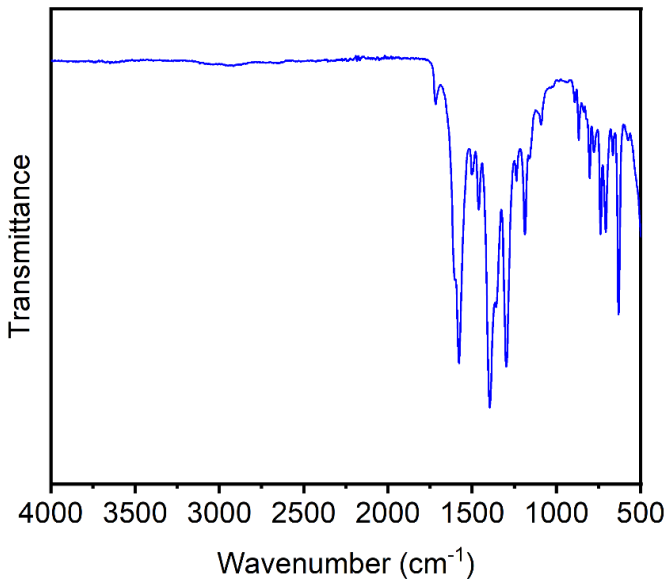

Figure S7. ATR IR spectrum of acetone-solvated Mg_2(*m*-dobdc)-ST prepared under solvothermal conditions.

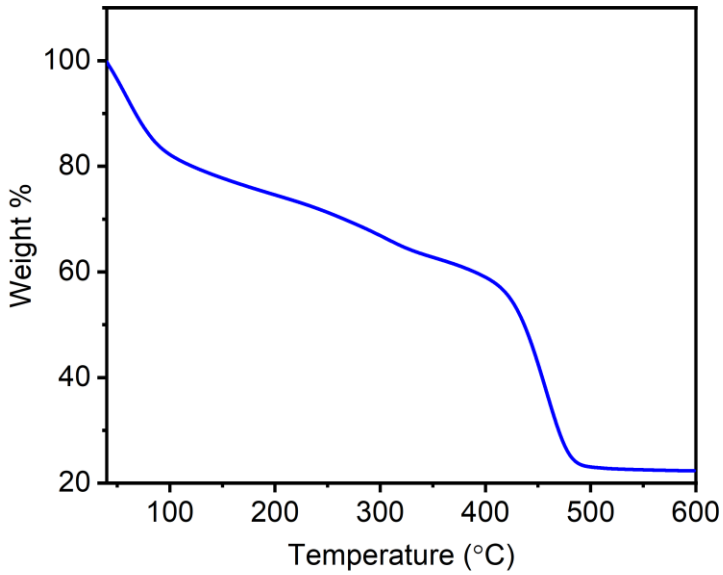

Figure S8. Thermogravimetric decomposition profile under N_2 of acetone-solvated Mg_2(*m*-dobdc)-ST prepared under solvothermal conditions.

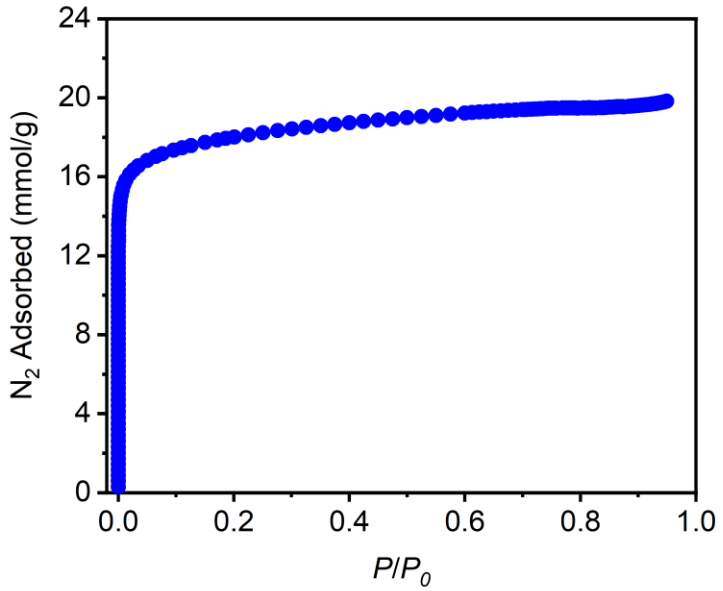

Figure S9. 77 K N_2 adsorption isotherm of activated Mg_2(*m*-dobdc)-ST prepared under solvothermal conditions. Fitting the data yielded a BET surface area of 1556 ± 2 m^2/g and a Langmuir surface area of 1971 ± 3 m^2/g. Note: (re-)activation of Mg_2(*m*-dobdc) at ramp rates faster than 1 °C/min consistently produced lower surface areas, likely due to partial pore collapse.[1]

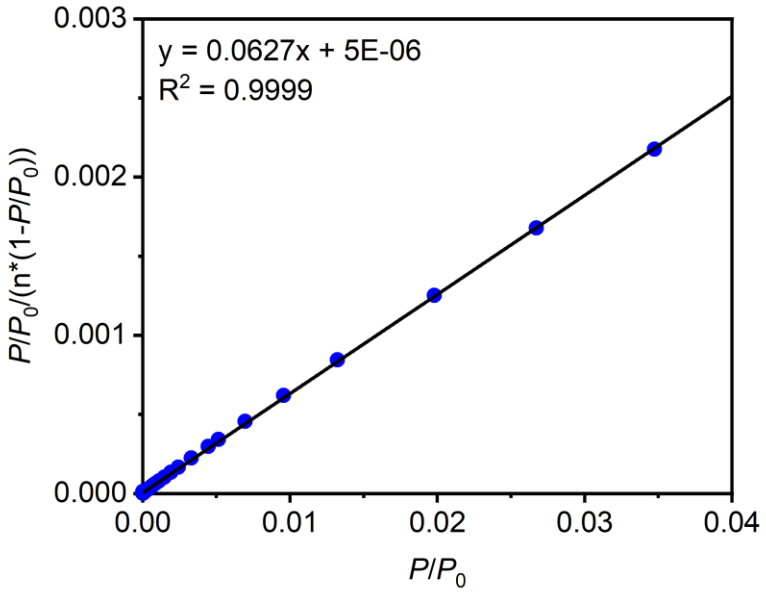

Figure S10. Linearized BET plot for the data in Figure S9.

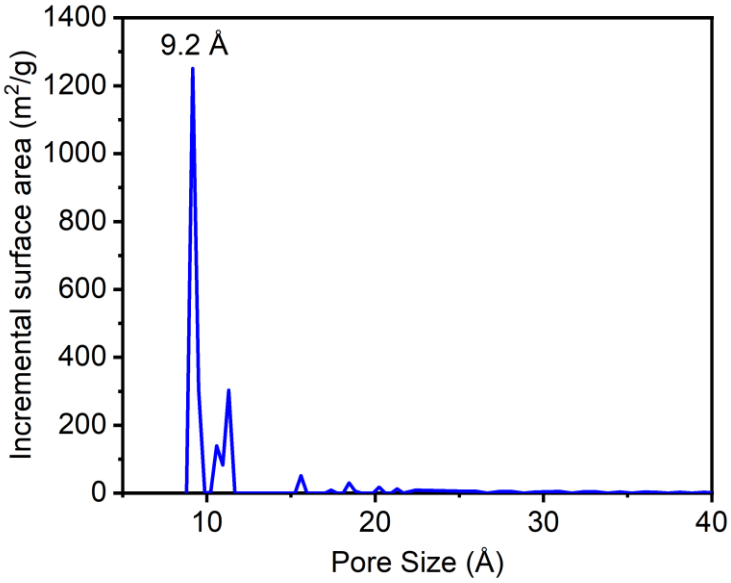

Figure S11. Density functional theory-calculated pore size distribution for Mg_2(*m*-dobdc)-ST prepared under solvothermal conditions, assuming a cylindrical pore shape with a metal oxide surface.

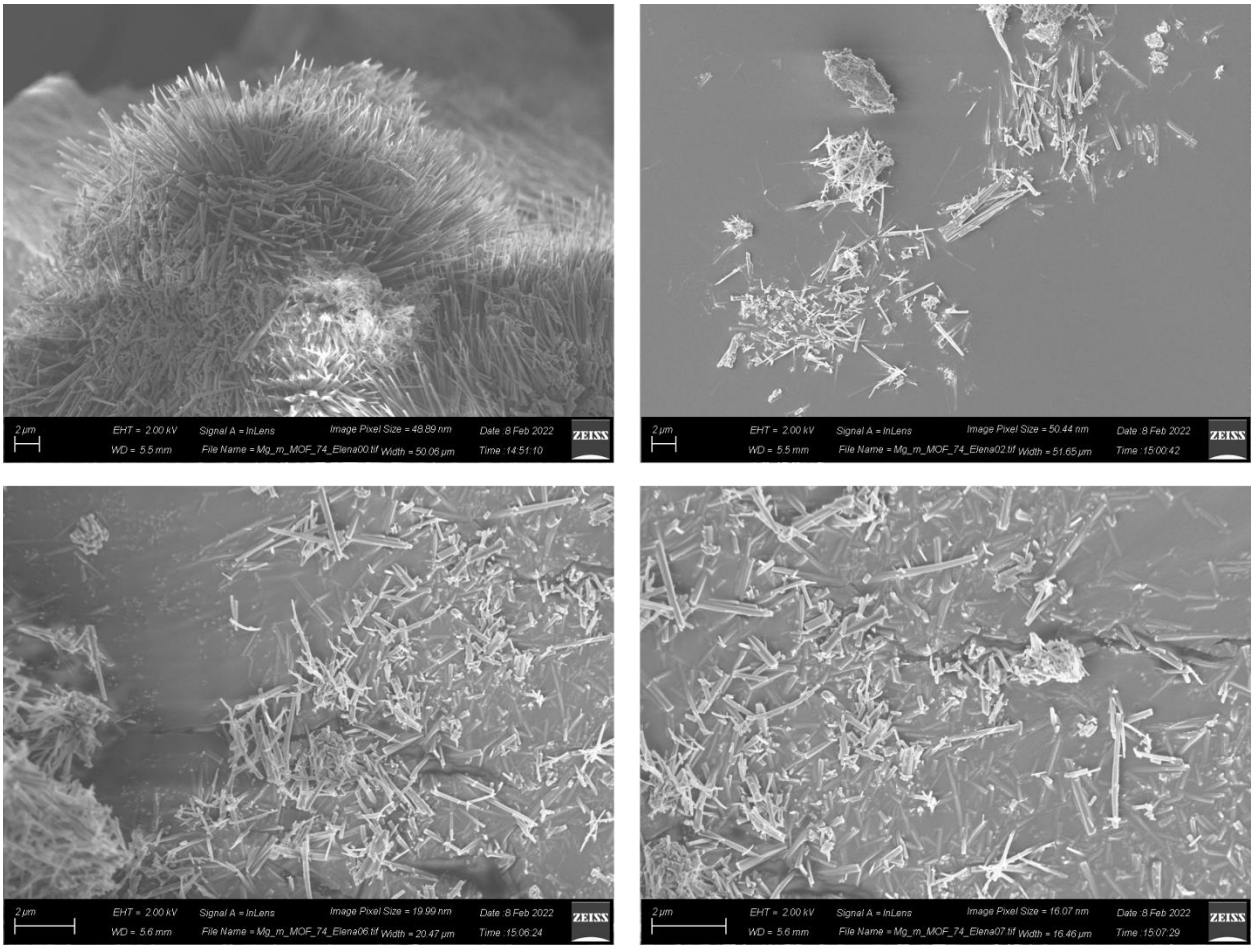

Figure S12. SEM images of Mg_2(*m*-dobdc)-ST prepared under solvothermal conditions.

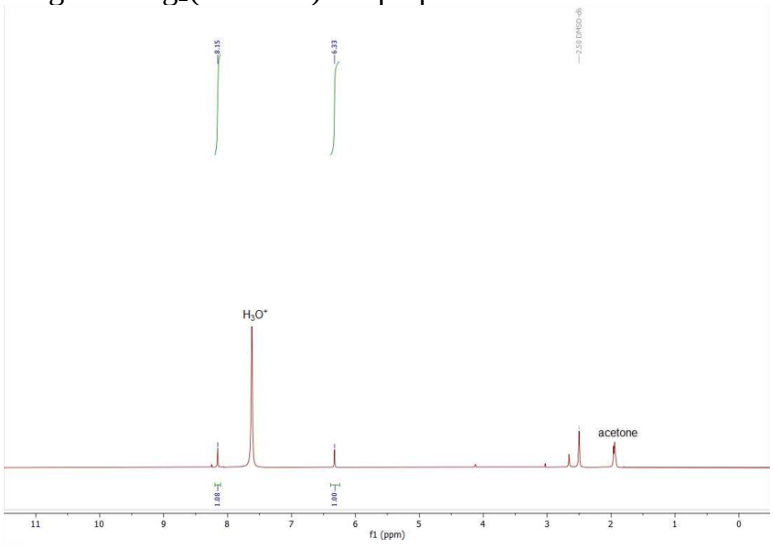

Figure S13. ^{1}H NMR (400 MHz, DMSO-d_6) spectrum of acetone-solvated Mg_2(*m*-dobdc)-ST digested with a 35 wt % DCl in D_2O solution. Only H_4*m*-dobdc and trace residual solvents (not DMF) are present.

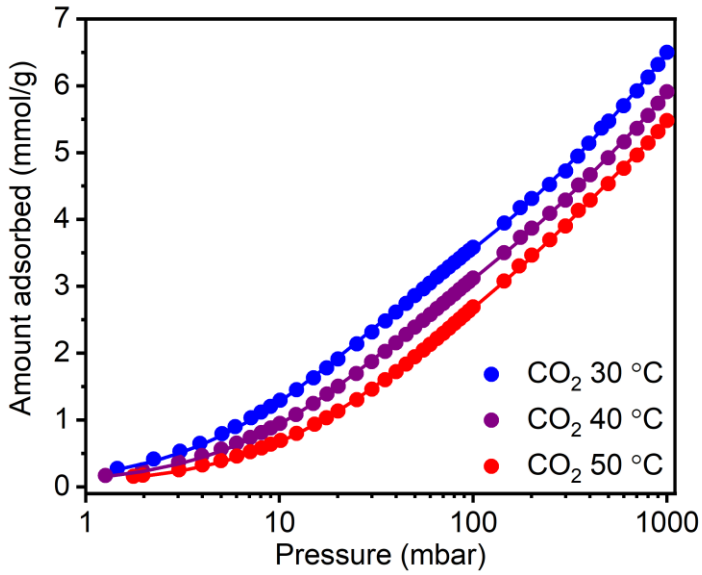

Figure S14. CO_2 adsorption isotherms at 30 °C (blue), 40 °C (purple), and 50 °C (red) for Mg_2(*m*-dobdc)-ST prepared under solvothermal conditions plotted on a logarithmic scale. The lines correspond to individual fits to the dual-site Langmuir model. A data point was considered equilibrated when <0.01% pressure change occurred over a 30 s interval. The sample was reactivated at 180 °C for >4 h under high vacuum (<10 μbar) between isotherms.

Table S2. Langmuir fit parameters determined from the independent fits in Figure S14 or from simultaneous fits to the dual-site Langmuir model for CO_2 adsorption in Mg_2(*m*-dobdc)-ST prepared under solvothermal conditions.

	30 °C	40 °C	50 °C	Simultaneous
$Q_{sat}1$ (mmol/g)	3.562387813	3.299342495	2.954564311	5.27463508
S1 (in multiples of R)	0.00253983	0.002539961	0.002540084	10.6874703
E1 (kJ/mol)	9.948367236	9.370755752	8.782091805	27.7162161
V1	1	1	1	1
$Q_{sat}2$ (mmol/g)	5.537449622	4.903756992	4.506572941	3.44815083
S2 (in multiples of R)	0.074038927	0.616263689	0.551761337	10.852239
E2 (kJ/mol)	0.557778332	2.037498801	2.287089469	37.4268706
V2	1	1	1	1
R^2	0.999833604	0.999859376	0.999861773	0.99966551

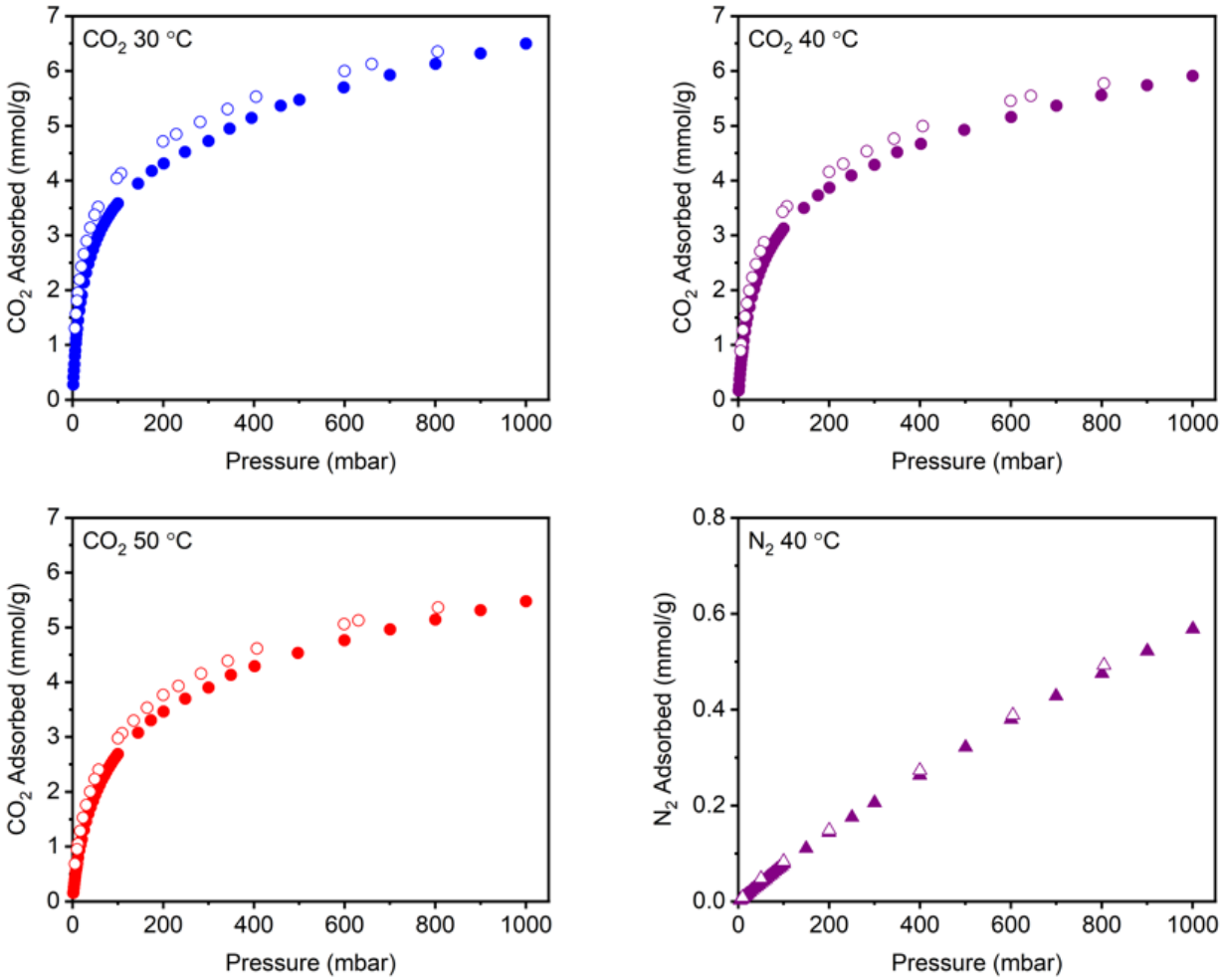

Figure S15. CO_2 adsorption (filled circles) and desorption (open circles) isotherms at 30 °C, 40 °C, and 50 °C, along with N_2 adsorption (filled triangles) and desorption (open triangles) at 40 °C, for Mg_2(*m*-dobdc)-ST prepared under solvothermal conditions. A data point was considered equilibrated when <0.01% pressure change occurred over a 30 s interval. The sample was reactivated at 180 °C for >4 h under high vacuum (<10 μbar) between isotherms. The adsorption data are included in main text Figure 6.

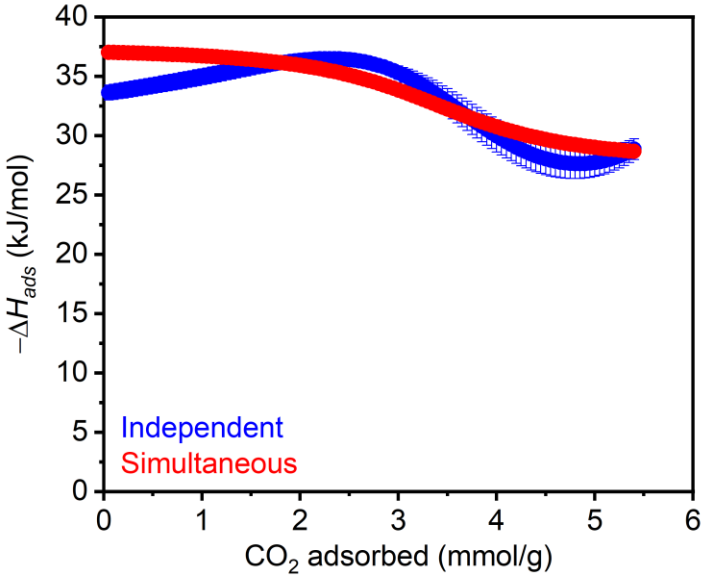

Figure S16. Heats of CO_2 adsorption ($-\Delta H_{ads}$) as a function of uptake in Mg_2(*m*-dobdc)-ST prepared under solvothermal conditions. The results from both independent and simultaneous fits to the dual-site Langmuir model are shown. The data for the simultaneous fits are included in main text Figure 6. Error bars are included and are too small to see in some cases.

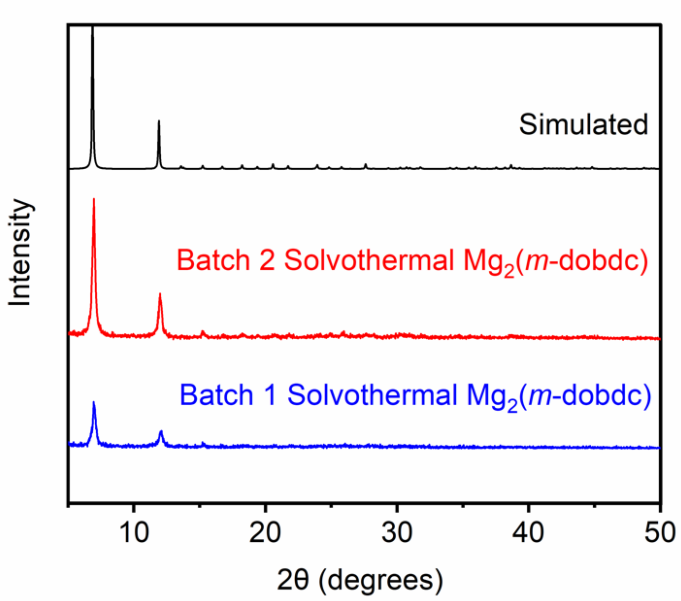

Figure S17. PXRD patterns (λ = 1.5406 Å) of two separate batches of acetone-solvated Mg_2(*m*-dobdc)-ST prepared under the optimized solvothermal conditions, confirming the reproducibility of this procedure. The simulated pattern based on the previously reported single-crystal X-ray diffraction structure of the isostructural framework Co_2(*m*-dobdc) is included for reference.[6]

4. Synthesis and characterization of mechanochemical (MC) Mg_2(*m*-dobdc)-MC.

a. Optimization of mechanochemical Mg_2(*m*-dobdc)-MC synthesis.

Procedure for small-scale mechanochemical reactions (Table S3). Small-scale syntheses were performed in 25 mL tungsten carbide vessels, using twelve tungsten carbide balls (ϕ = 2.0 mm) in each vessel, with a Fritsch Pulverisette 7 ball mill (two vessels were used per synthesis). Each vessel was charged with H_4*m*-dobdc (49.5 mg, 0.250 mmol, 1.00 equiv.), metal salt (0.750 mmol, 3.00 equiv.), and organic base (1.10 mmol, 4.40 equiv.), as indicated in Table S3. The reaction mixture was then milled at 600 rpm for either 1, 5, or 10 min as indicated in Table S3. The product was rinsed out with methanol (15 mL) and filtered, using sonication as needed to remove the product from the vessel. PXRD patterns were collected on freshly-washed solids. The tested conditions are based on those previously reported for the preparation of M_2(dobdc) MOFs under mechanochemical conditions.[1,7]

Table S3. Mechanochemical Mg_2(*m*-dobdc)-MC synthesis attempts.

Condition	Base	Time (min)	Salt	Result
1	Hünig's base	1	$Mg(NO_3)_2{\cdot}6H_2O$	Pink solid, incorrect phase
2		5		Pink-brown solid, amorphous solid
3		10		Pink-brown, incorrect phase
4	Et_3N	1		Pink, amorphous solid
5		5		Gray solid, Mg_2(*m*-dobdc)
6		10		Gray solid, Mg_2(*m*-dobdc)
7		5	$Mg(OAc)_2{\cdot}4H_2O$	Gray solid, Mg_2(*m*-dobdc)
8		5	MgO	Pink solid, MgO
9	2,6-lutidine	5	$Mg(NO_3)_2{\cdot}6H_2O$	No solid

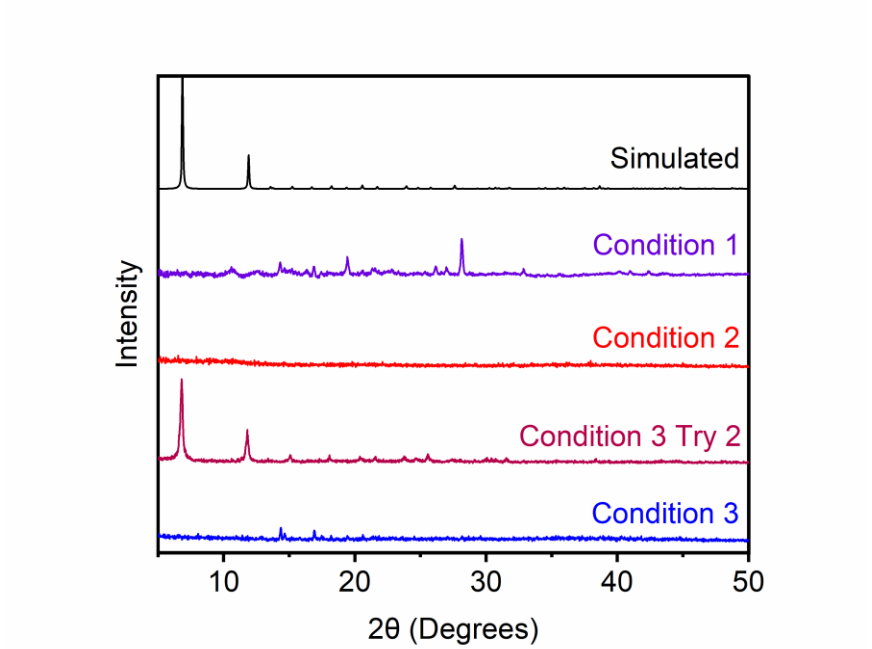

Figure S18. PXRD patterns (λ = 1.5406 Å) of mechanochemical Mg_2(*m*-dobdc)-MC synthesis attempts using Hünig's base. The previously reported method (Condition 3) was found to be modestly reproducible.[1] The simulated pattern based on the previously reported single-crystal X-ray diffraction structure of the isostructural framework Co_2(*m*-dobdc) is included for reference.[6]

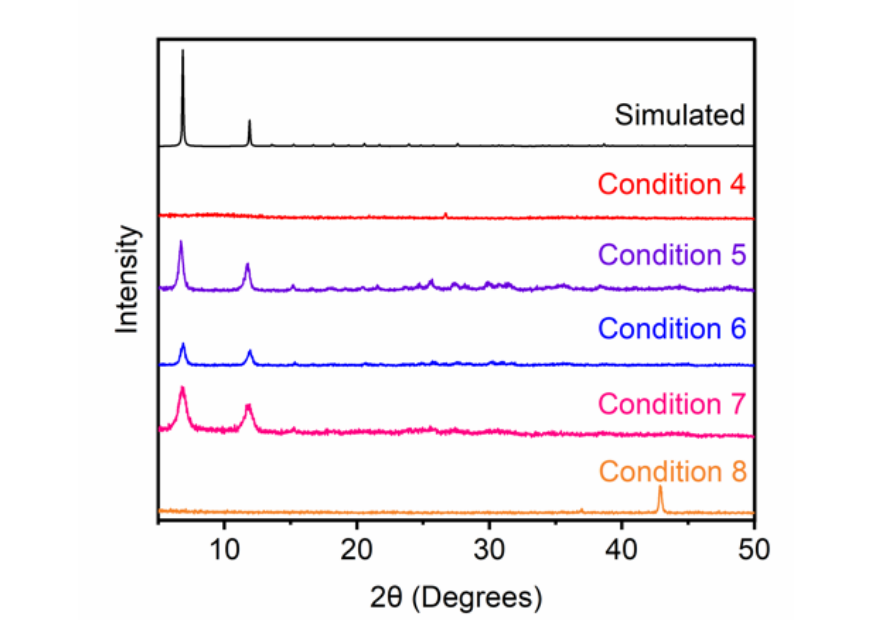

Figure S19. PXRD patterns (λ = 1.5406 Å) of mechanochemical Mg_2(*m*-dobdc)-MC synthesis attempts using Et_3N. Conditions 5 and 6 (Table S3) yielded the highest quality material and thus Condition 6 was employed for large-scale synthesis of Mg_2(*m*-dobdc)-MC. The simulated pattern based on the previously reported single-crystal X-ray diffraction structure of the isostructural framework Co_2(*m*-dobdc) is included for reference.[6]

b. Large-scale synthesis of mechanochemical Mg_2(*m*-dobdc)-MC.

Procedure for large-scale mechanochemical synthesis. Two 25 mL tungsten carbide vessels filled with twelve tungsten carbide balls (ϕ = 2.0 mm) were each charged with H_4*m*-dobdc (198 mg, 1.00 mmol, 1.00 equiv.), $Mg(NO_3)_2 \cdot 6H_2O$ (768 mg, 3.00 mmol, 3.00 equiv.), and Et_3N (0.612 mL, 4.40 mmol, 4.40 equiv.). The reaction mixtures were then milled at 600 rpm for 10 min. The product was rinsed out with methanol (50 mL) and filtered, using sonication as needed to remove the product from the vessels. The gray-white solid was transferred to a 500 mL Pyrex jar. MeOH (250 mL) was added, and the jar was placed in an oven that had been pre-heated to 60 °C. The jar was allowed to stand at 60 °C for 24 h. At this time, the jar was allowed to cool to room temperature, and the MeOH was decanted. Fresh MeOH (250 mL) was added, and the jar was returned to the oven. This process was repeated for a total of two hot MeOH washes. After decanting the final MeOH wash, acetone (250 mL) was added to the jar, and the jar was allowed to stand at room temperature. The soaking process outlined above was repeated for a total of two room temperature acetone washes. After the final acetone wash was decanted, the solid was transferred to a 10 mL Schlenk flask and activated under high vacuum (<100 mbar) at 180 °C in a sand bath (ramp rate 1 °C/min) for 24 h to yield activated Mg_2(*m*-dobdc) (459 mg, 95% yield) as an off-white solid. Approximately 50 mg of MOF was transferred to a Micromeritics ASAP tube and activated under high vacuum (<10 μbar) at 180 °C for 24 h prior to gas sorption measurements.

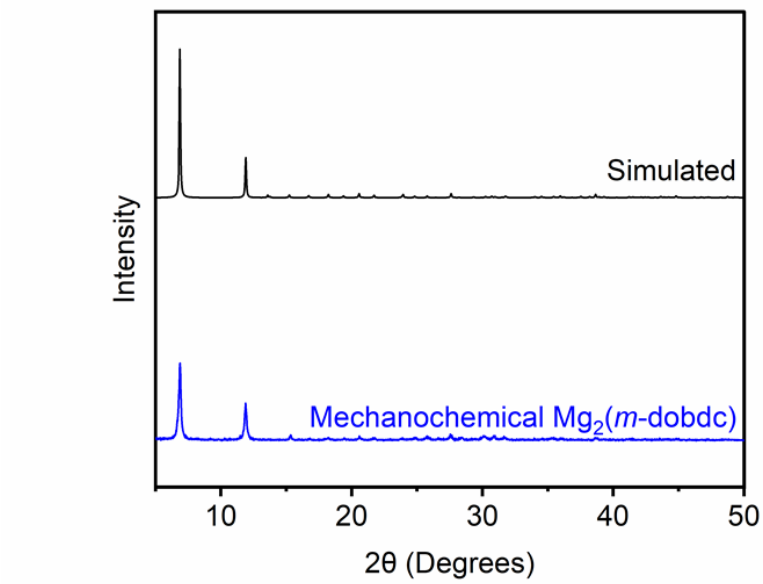

Figure S20. PXRD pattern (λ = 1.5406 Å) of acetone-solvated Mg_2(*m*-dobdc)-MC prepared under mechanochemical conditions. The simulated pattern based on the previously reported single-crystal X-ray diffraction structure of the isostructural framework Co_2(*m*-dobdc) is included for reference.[2]

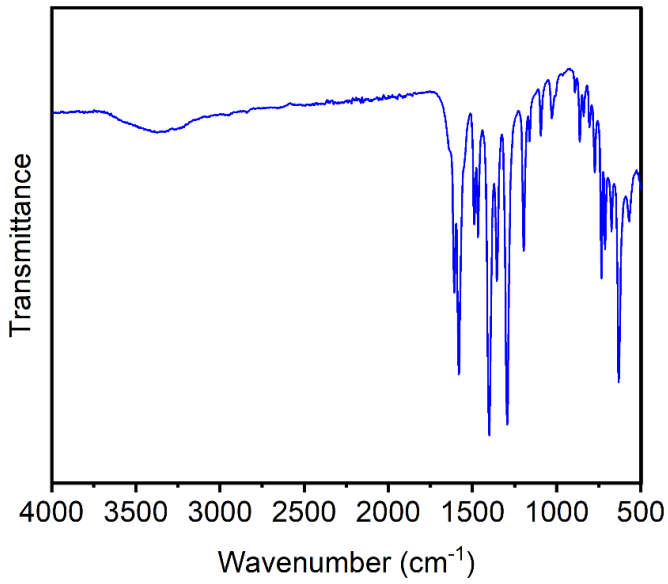

Figure S21. ATR IR spectrum of acetone-solvated Mg_2(*m*-dobdc)-MC prepared under mechanochemical conditions.

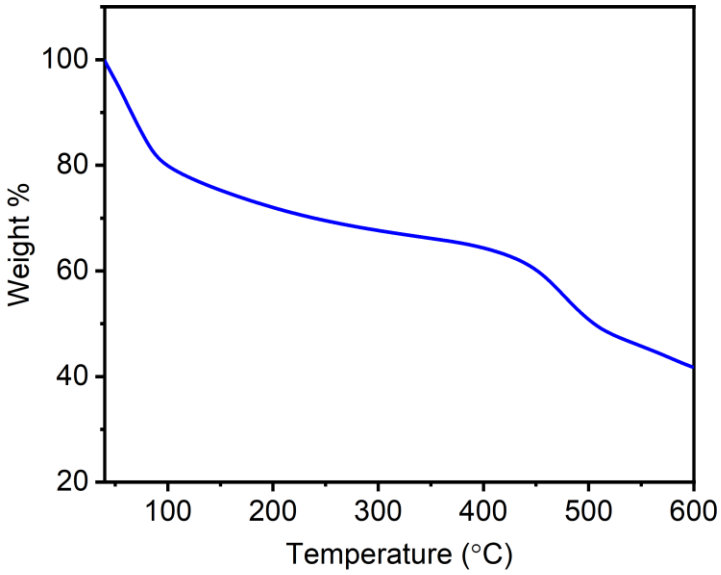

Figure S22. Thermogravimetric decomposition profile under N_2 of acetone-solvated Mg_2(*m*-dobdc)-MC prepared under mechanochemical conditions.

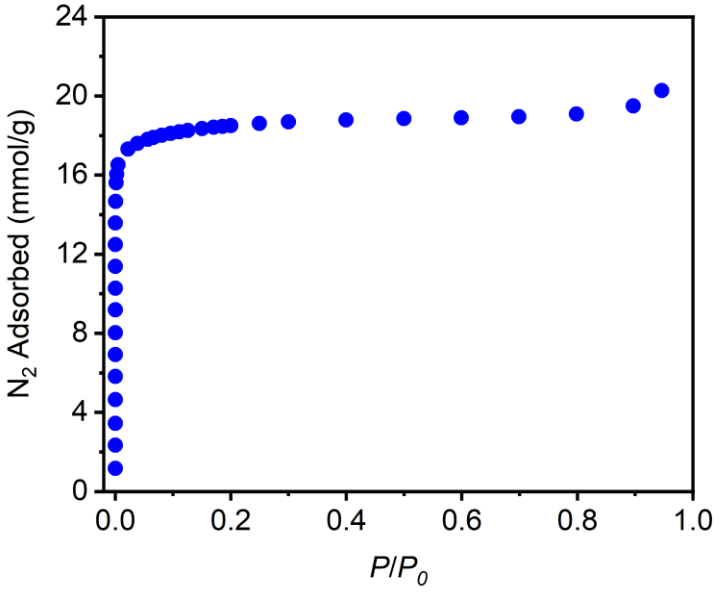

Figure S23. 77 K N_2 adsorption (filled circles) and desorption (open circles) isotherm of activated Mg_2(*m*-dobdc)-MC prepared under mechanochemical conditions. Fitting the data yielded a BET surface area of 1653 ± 2 m^2/g and a Langmuir surface area of 1964 ± 38 m^2/g.

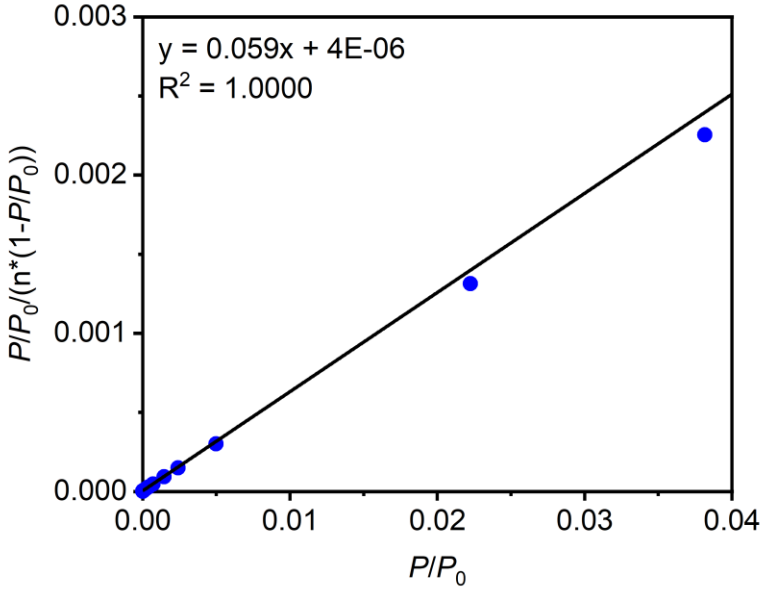

Figure S24. Linearized BET plot for the data in Figure S23.

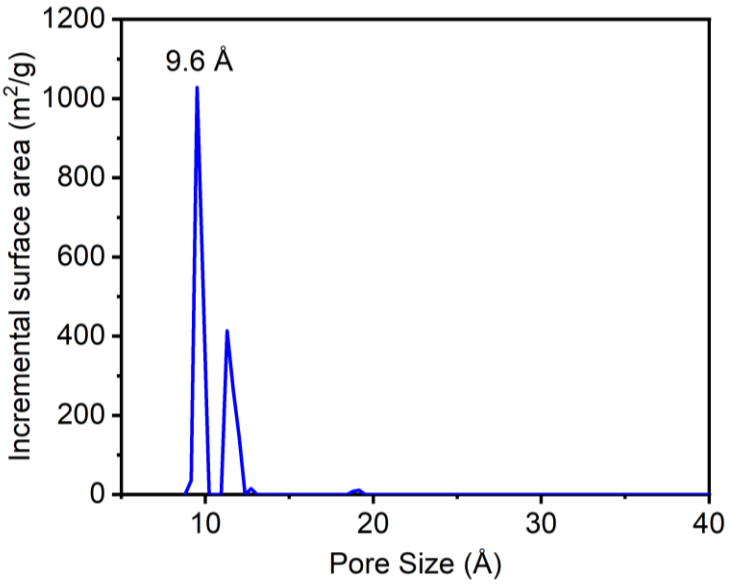

Figure S25. Density functional theory-calculated pore size distribution for Mg_2(*m*-dobdc)-MC prepared under mechanochemical conditions, assuming a cylindrical pore shape with a metal oxide surface.

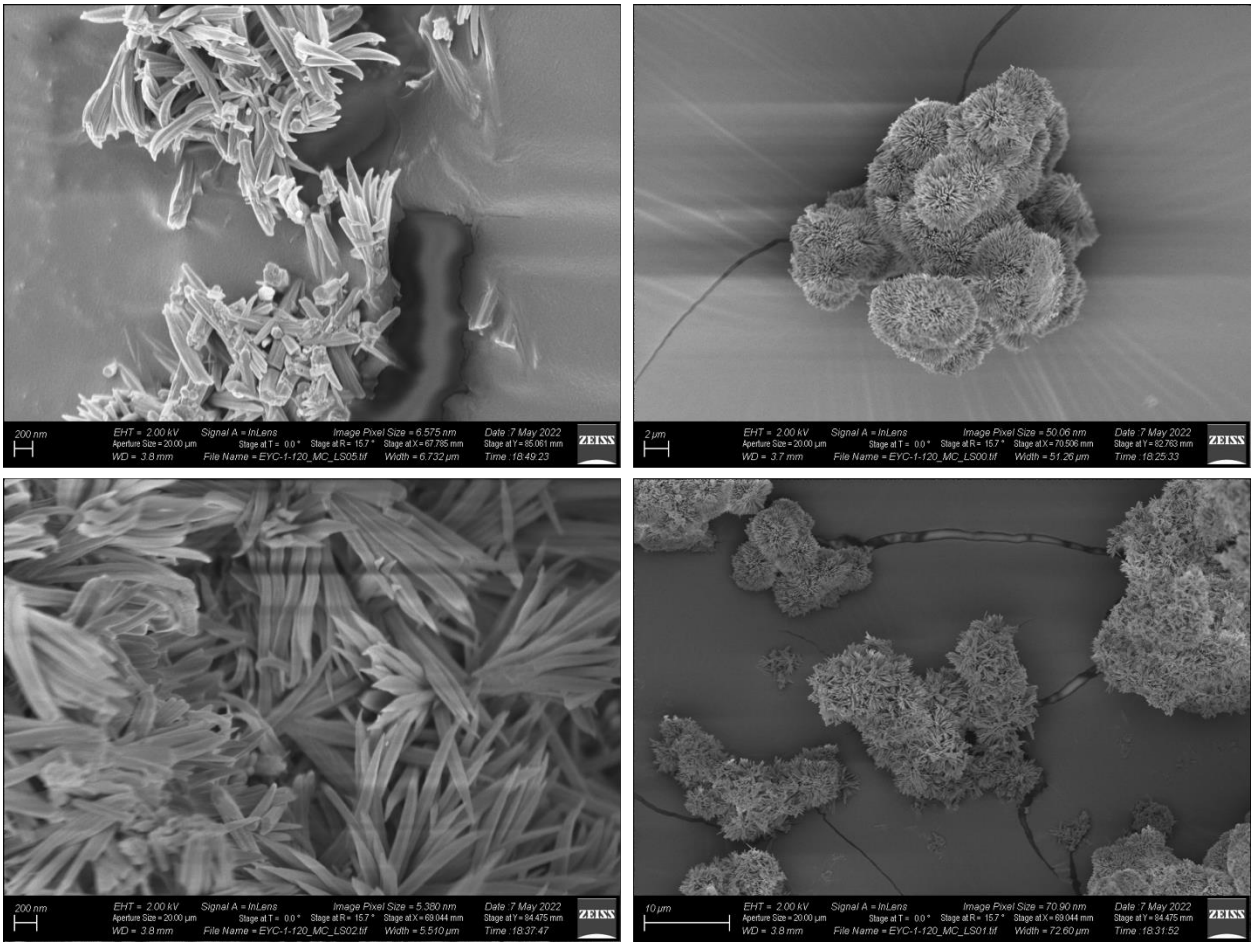

Figure S26. SEM images of Mg_2(*m*-dobdc)-MC prepared under mechanochemical conditions.

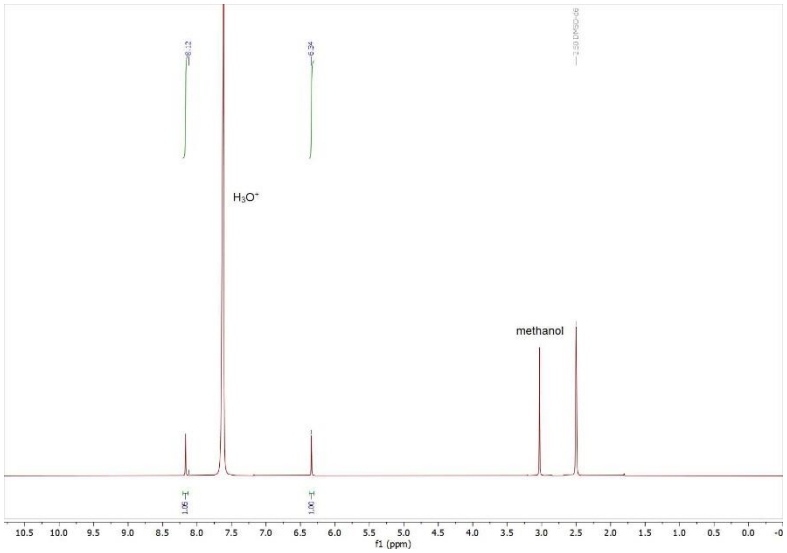

Figure S27. ^{1}H NMR (400 MHz, DMSO-d_6) spectrum of acetone-solvated Mg_2(*m*-dobdc)-MC digested with a 35 wt % DCl in D_2O solution. Only H_4*m*-dobdc and trace residual solvents (not DMF) are present.

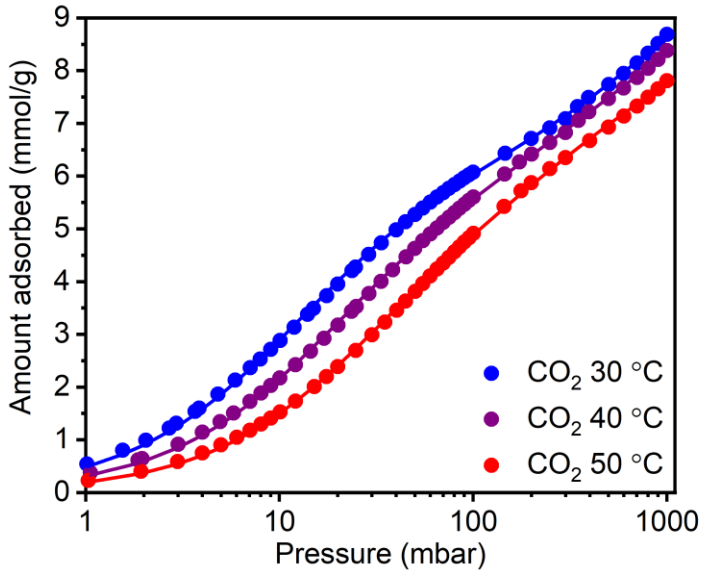

Figure S28. CO_2 adsorption isotherms at 30 °C (blue), 40 °C (purple), and 50 °C (red) for Mg_2(*m*-dobdc)-MC prepared under mechanochemical conditions plotted on a logarithmic scale. The lines correspond to individual fits to the dual-site Langmuir model. A data point was considered equilibrated when <0.01% pressure change occurred over a 30 s interval. The sample was reactivated at 180 °C for >4 h under high vacuum (<10 μbar) between isotherms.

Table S4. Langmuir fit parameters determined from the independent fits in Figure S28 or from simultaneous fits to the dual-site Langmuir model for CO_2 adsorption in Mg_2(*m*-dobdc)-MC prepared under mechanochemical conditions.

	30 °C	40 °C	50 °C	Simultaneous
$Q_{sat}1$ (mmol/g)	6.249672064	5.996773132	5.584896351	4.39224907
S1 (in multiples of R)	0.002539467	0.00253981	0.002539927	9.31281549
E1 (kJ/mol)	11.15776285	10.38790032	9.529107367	24.3764317
V1	1	1	1	1
$Q_{sat}2$ (mmol/g)	4.927522435	4.207318497	3.59367734	6.1147741
S2 (in multiples of R)	0.088861794	0.556343845	0.464706246	12.4317063
E2 (kJ/mol)	0.227614138	2.268732197	2.821630884	42.613078
V2	1	1	1	1
R^2	0.999636071	0.999709461	0.999704503	0.99931636

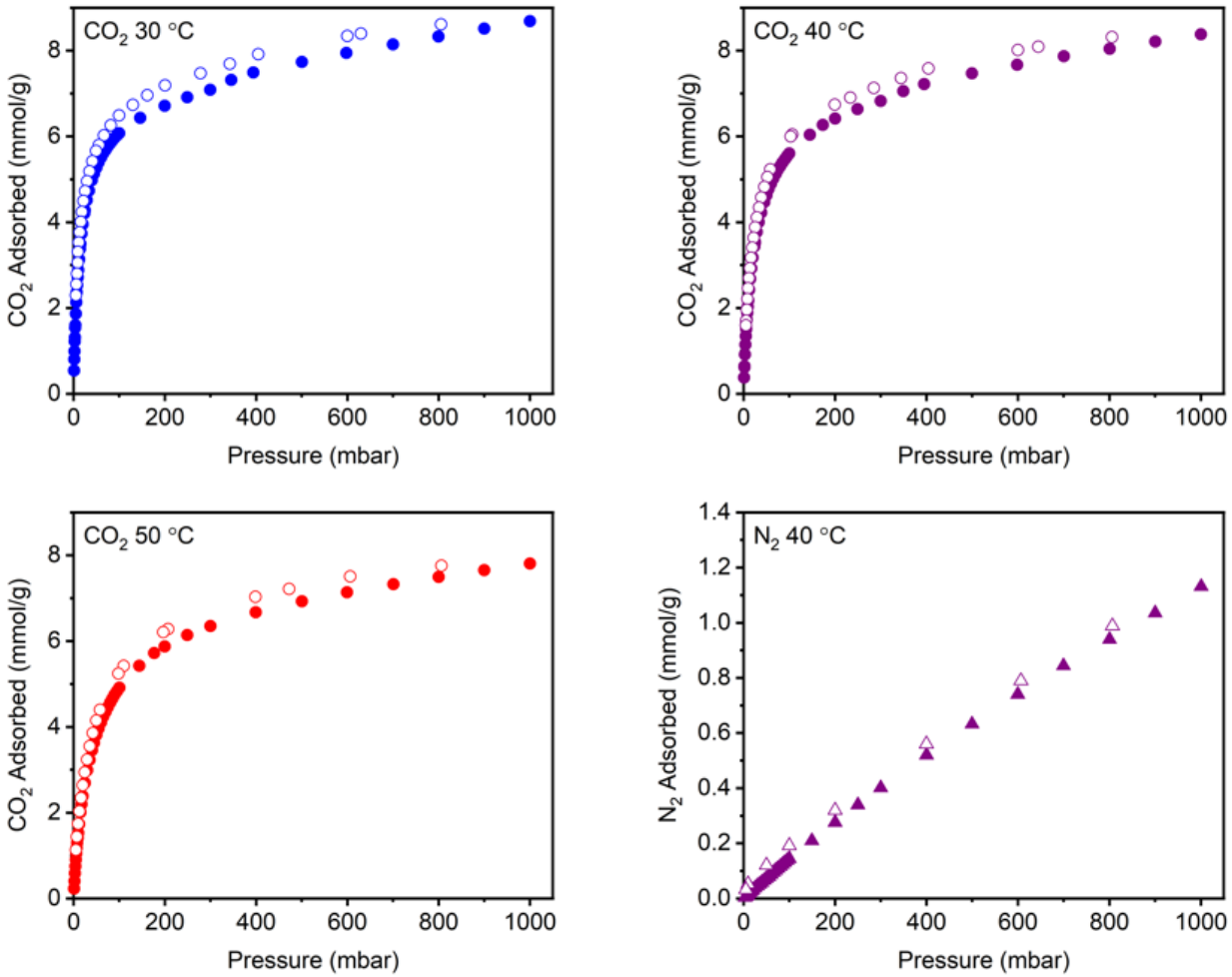

Figure S29. CO_2 adsorption (filled circles) and desorption (open circles) isotherms at 30 °C, 40 °C, and 50 °C, along with N_2 adsorption (filled triangles) and desorption (open triangles) at 40 °C, for Mg_2(*m*-dobdc)-MC prepared under mechanochemical conditions. A data point was considered equilibrated when <0.01% pressure change occurred over a 30 s interval. The sample was reactivated at 180 °C for >4 h under high vacuum (<10 μbar) between isotherms. The adsorption data are included in main text Figure 6.

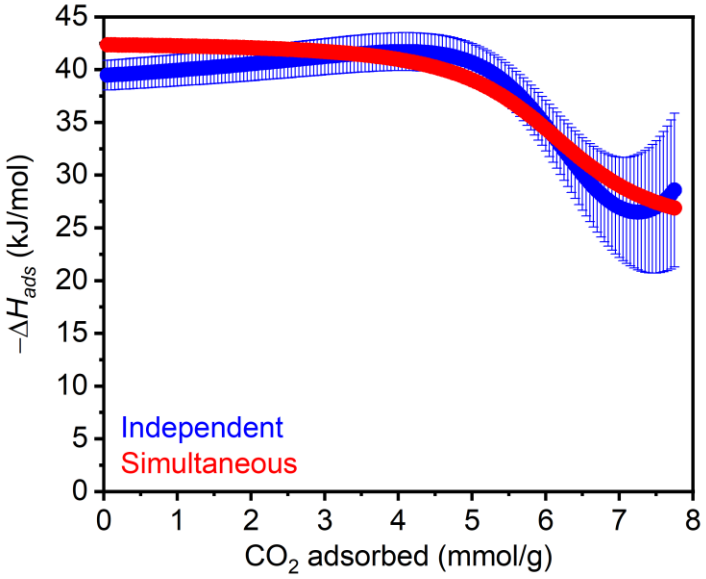

Figure S30. Heats of CO_2 adsorption ($-\Delta H_{ads}$) as a function of uptake in Mg_2(*m*-dobdc)-MC prepared under mechanochemical conditions. The results from both independent and simultaneous fits to the dual-site Langmuir model are shown. The data for the simultaneous fits are included in main text Figure 6. Error bars are included and are too small to see in some cases.

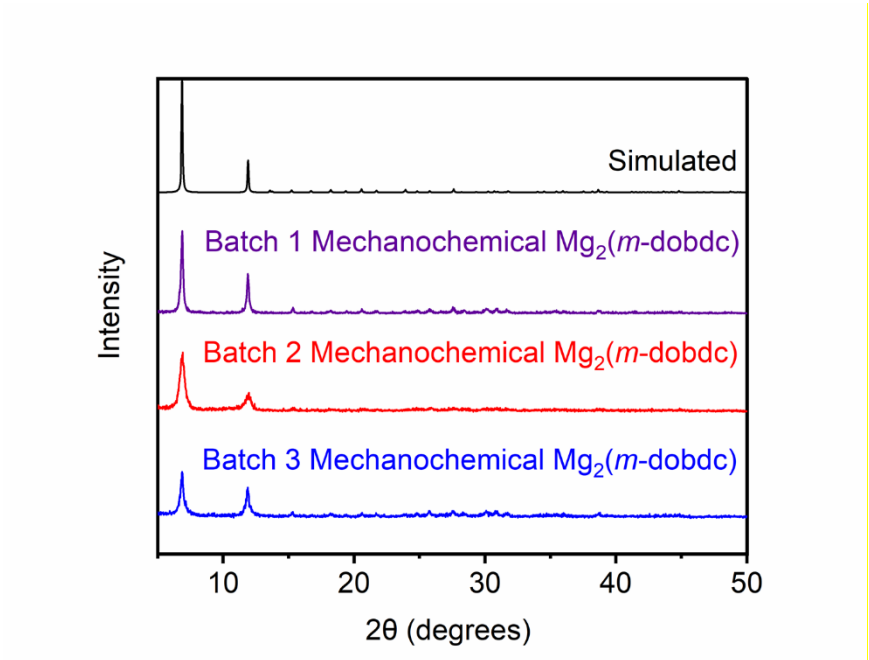

Figure S31. PXRD patterns (λ = 1.5406 Å) of three separate batches of acetone-solvated Mg_2(*m*-dobdc)-MC prepared under the optimized mechanochemical conditions, confirming the reproducibility of this procedure. The simulated pattern based on the previously reported single-crystal X-ray diffraction structure of the isostructural framework Co_2(*m*-dobdc) is included for reference.[6]

5. References.

(1) Wang, Z.; Li, Z.; Ng, M.; Milner, P. J. Rapid Mechanochemical Synthesis of Metal–Organic Frameworks Using Exogenous Organic Base. *Dalton Trans.* **2020**, *49* (45), 16238–16244. https://doi.org/10.1039/D0DT01240H.

(2) Colwell, K. A.; Jackson, M. N.; Torres-Gavosto, R. M.; Jawahery, S.; Vlaisavljevich, B.; Falkowski, J. M.; Smit, B.; Weston, S. C.; Long, J. R. Buffered Coordination Modulation as a Means of Controlling Crystal Morphology and Molecular Diffusion in an Anisotropic Metal–Organic Framework. *J. Am. Chem. Soc.* **2021**, *143* (13), 5044–5052. https://doi.org/10.1021/jacs.1c00136.

(3) Garzón-Tovar, L.; Carné-Sánchez, A.; Carbonell, C.; Imaz, I.; Maspoch, D. Optimised Room Temperature, Water-Based Synthesis of CPO-27-M Metal–Organic Frameworks with High Space-Time Yields. *J. Mater. Chem. A* **2015**, *3* (41), 20819–20826. https://doi.org/10.1039/C5TA04923G.

(4) Queen, W. L.; Hudson, M. R.; Bloch, E. D.; Mason, J. A.; Gonzalez, M. I.; Lee, J. S.; Gygi, D.; Howe, J. D.; Lee, K.; Darwish, T. A. Comprehensive Study of Carbon Dioxide Adsorption in the Metal–Organic Frameworks M_2(dobdc) (M= Mg, Mn, Fe, Co, Ni, Cu, Zn). *Chem. Sci.* **2014**, *5* (12), 4569–4581.

(5) Tranchemontagne, D. J.; Hunt, J. R.; Yaghi, O. M. Room Temperature Synthesis of Metal-Organic Frameworks: MOF-5, MOF-74, MOF-177, MOF-199, and IRMOF-0. *Tetrahedron* **2008**, *64* (36), 8553–8557. https://doi.org/10.1016/j.tet.2008.06.036.

(6) Bachman, J. E.; Kapelewski, M. T.; Reed, D. A.; Gonzalez, M. I.; Long, J. R. M_2 (*m*-Dobdc) (M = Mn, Fe, Co, Ni) Metal–Organic Frameworks as Highly Selective, High-Capacity Adsorbents for Olefin/Paraffin Separations. *J. Am. Chem. Soc.* **2017**, *139* (43), 15363–15370. https://doi.org/10.1021/jacs.7b06397.

(7) Ayoub, G.; Karadeniz, B.; Howarth, A. J.; Farha, O. K.; Đilović, I.; Germann, L. S.; Dinnebier, R. E.; Užarević, K.; Friščić, T. Rational Synthesis of Mixed-Metal Microporous Metal–Organic Frameworks with Controlled Composition Using Mechanochemistry. *Chem. Mater.* **2019**, *31* (15), 5494–5501. https://doi.org/10.1021/acs.chemmater.9b01068.